AMSI VACATION RESEARCH SCHOLARSHIPS 2019–20

EXPLORE THE MATHEMATICAL SCIENCES THIS SUMMER

Generalisations of the Cohan Circle Puzzle in Investigating the Geometry of Piecewise Isometries

Martin Gossow

Supervised by Dr. Lachlan Smith and Prof. Georg Gottwald

The University of Sydney

Vacation Research Scholarships are funded jointly by the Department of Education and the Australian Mathematical Sciences Institute.

AMSI AUSTRALIAN MATHEMATICAL SCIENCES INSTITUTE

Australian Government Department of Education

I owe much to Dr. Lachlan Smith for his supervision of this project. His ideas, corrections, and encouragement shaped both my work and my methodology in research. I want to further extend this thanks to Prof. Georg Gottwald and the University of Sydney mathematics department. I want to thank the Australian Mathematical Sciences Institute and the Department of Education for allowing this project to happen through their planning and funding. Finally, those friends I made at the 'AMSI Connect' event for their thought-provoking questions, observations, and friendliness which encourage me to approach my study of mathematics with evermore joyous determination.

Contents

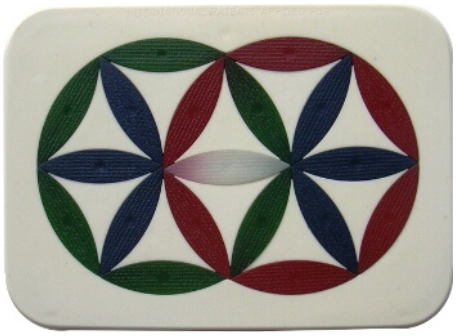

The Cohan Circle Puzzle [Nortmann, 2002]

Abstract

This report investigates the properties of piecewise isometries through the explicit study of one particular system; overlapping disc rotations. Piecewise isometries describe cutting and shuffling behaviour, such as shuffling a deck of cards or mixing a twisty puzzle: such as a Rubik's cube. These systems are fundamentally different to smooth dynamical systems often associated with mixing. They may arise naturally in mathematical studies of combinatorics, group theory, dynamics and numerical computation. A key feature of these systems is the exceptional set, which gives the points cut by the transformation. The exceptional set elucidates the transport properties of the dynamics, and is an important tool in studying the mixing of these systems. We give some fundamental definitions for piecewise isometries and prove various properties about the exceptional set for the Cohan puzzle and its generalisations, including an analogue into three dimensions. Finally, we work towards a conjecture concerning the cardinality of cells, the regions of non-mixing that remain after removing the exceptional set.

1 Introduction

A transformation refers to a bijective map $T : D \to D$, for some $D \subseteq \mathbb{R}^n$. Such a transformation is an isometry if $\forall x, y \in D$, then $d(x, y) = d(T(x), T(y))$, where d is the standard Euclidean metric. A *piecewise isometry* is a generalisation of this idea [Goetz, 2000]. Suppose we can decompose our domain D into finite, non-intersecting components A_k, for $k \in \{1, \ldots, n\}$, such that T acts as an isometry on each A_k. Then T is a piecewise isometry and each A_k is referred to as an atom of our transformation [Goetz, 2003].

Restricting to an atom, the transformation is an isometry, which implies continuity. On the boundary of atoms however, we may get points where the transformation is not continuous [Krotter et al., 2012]. The collection of these points of discontinuity give the exceptional set $\mathcal{E}_T := \{x \in D \,|\, T^n \text{ discontinuous at } x \text{ for some } n \in \mathbb{Z}\}$ [Smith et al., 2019]. This includes both forward and backward iterations of our transformation. If we only allow $n \in \mathbb{N}$, we get the forward exceptional set $\mathcal{E}_T^+$. Suppose we have a set of transformations $\{T_1, \ldots, T_m\}$, such that for each $k \in \{1, \ldots, m\}$, there are domains $D_k \subseteq D$ such that $T_k : D_k \to D_k$ are piecewise isometries. Let $\mathbb{T} = \{T_1, \ldots, T_m\}^*$ be the set of all (possibly infinite) sequences of these transformations. We then define the full exceptional set $\mathbf{E}_\mathbb{T} := \bigcup_{T \in \mathbb{T}} \mathcal{E}_T$. The set $D \setminus \mathcal{E}_T$ or $D \setminus \mathbf{E}_\mathbb{T}$ is known as the normal set. When the exceptional set is removed, we are left with a collection of islands, which are maximally connected subsets of the normal set. These islands may have Euclidean measure zero, in which case they are known as degenerate.

As well as studying the nature of the exceptional set $\mathcal{E}$, we want to consider what happens to points in the normal set $D \setminus \mathcal{E}$. To this, we can look at the *itinerary* of a point. After indexing the atoms of our transformation, the itinerary of a point is the sequence of atoms $T^n(z)$ visits. The itinerary gives us the sequence of isometries experienced by z and hence its images. Sets of points with the same itinerary are called cells [Goetz, 2003].

Statement of Authorship. Under the direction of my supervisor Dr. Smith, I wrote Python code to generate the images of the exceptional sets shown, proved the lemmas stated and drafted this report. Dr. Smith advised me in interpreting the images, providing direction of study and in proofreading.

2 Overlapped Disc Rotations

Overlapped disc rotations consist of two adjacent discs, such that the interior of each of the discs can be independently rotated [Smith et al., 2019]. The Cohan Circle puzzle is a specific example of this, where the two discs pass through each other's centres, and the rotations are $\pi/3$ radians [Nortmann, 2002]. As a result, the puzzle must be cut up into petals and triangles so that these rotations are possible. If we allow any sequence of rotations, then each petal and interior triangle become atoms of our puzzle. This report will explore overlapped disc rotations and properties of their exceptional set, the lines that must be cut to allow the puzzle to rotate.

Suppose the two rotating discs have centres 1 and -1, and both have radius 2. Our domain D is the union of these two discs. Supposing this domain exists in the complex plane (rather than $\mathbb{R}^2$), the rotation of the left and right discs are given respectively by the following transformations:

$$R_1^\theta(z) = \begin{cases} e^{i\theta}(z+1)-1, & |z+1| \le 2 \\ z, & \text{otherwise} \end{cases} \qquad R_2^\theta(z) = \begin{cases} e^{i\theta}(z-1)+1, & |z-1| \le 2 \\ z, & \text{otherwise} \end{cases}$$

Note: we call R_k^θ a rational rotation if $\theta \in \pi\mathbb{Q}$. We want to calculate the exceptional set $\mathcal{E}_T$ of this system for some transformation T, which will be a sequence of these rotations. Unless stated otherwise, we will be considering $T^\theta = R_2^\theta \circ R_1^\theta$. This transformation has three atoms (and three related isometries) given by

$$T^\theta(z) = \begin{cases} (R_2^\theta \circ R_1^\theta)(z), & |z+1| \le 2 \,\&\, |R_1^\theta(z) - 1| \le 2 \\ R_1^\theta(z), & |z+1| \le 2 \\ R_2^\theta(z), & |z-1| \le 2 \end{cases}$$

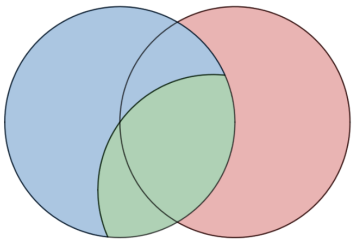

Figure 1: The atoms of T^θ, with the colours; 0 - Green, 1 - Blue, 2 - Red.

We can rephrase the first condition by $|z+1| \le 2 \,\&\, |z+1-2e^{-i\theta}| \le 2$. When choosing the transformation, we read down the cases and choose the first one that z satisfies. Hence, these atoms satisfy a disjoint union for D. We notate these atoms 0, 1 and 2 in their given order.

Lemma 2.1. *Suppose R_z^θ and R_ω^ϕ are two counter-clockwise rotations of angle θ and ϕ about the centres z and ω respectively. Let $R = R_\omega^\phi \circ R_z^\theta$ be the composition of the two rotations. If $\theta + \phi \in 2\pi\mathbb{Z}$, then R is a translation, else it is a rotation (with form given in the proof).*

Proof. It is known that the rotation R_z^θ can be written as $\sigma_m \circ \sigma_l$, where σ_l and σ_m are reflections about two lines l and m, such that the counter-clockwise angle from l to m is $\theta/2$ and both lines pass through z. We can do the same for $R_\omega^\phi = \sigma_o\sigma_n$. Let $m = n$ be the line passing from z to ω, as in Figure 2. Hence:

$$R_\omega^\phi \circ R_z^\theta = \sigma_o\sigma_n\sigma_m\sigma_l = \sigma_o\sigma_n^2\sigma_l = \sigma_o\sigma_l$$

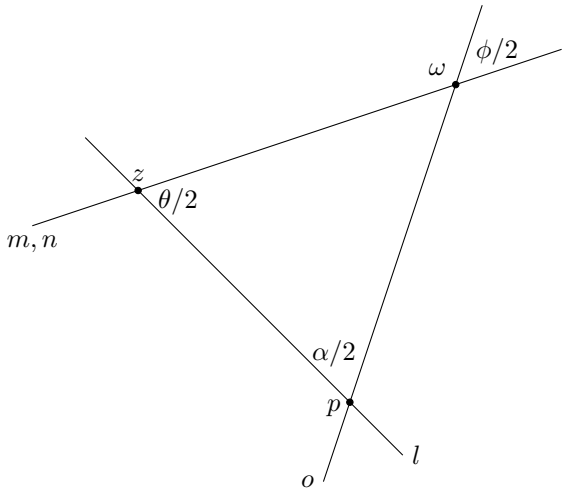

Figure 2: A diagram of the lines l, m, n, o to determine the composition of rotations

First suppose that $\theta/2+\phi/2 \in \pi\mathbb{Z}$, and hence $\theta+\phi = 2\pi\mathbb{Z}$. Then l and o are parallel and $\sigma_o\sigma_l$ is a translation by $2(\omega - z)$, or twice the perpendicular vector between the lines. Otherwise, the two lines l and o meet at some point p and make an angle of $\alpha/2$ as shown. Hence, $\sigma_o\sigma_l$ is a clockwise rotation of α about the point p. In our notation before, $\sigma_o\sigma_l = R_p^{-\alpha}$. From the properties of a triangle we have:

$$\frac{\theta}{2} + \frac{\phi}{2} + \frac{\alpha}{2} = \pi \implies \alpha = 2\pi - (\theta + \phi) \implies -\alpha = \theta + \phi - 2\pi$$

As $-\alpha$ is the counter-clockwise rotation angle, we consider $-\alpha \equiv \theta + \phi \pmod{2\pi}$.
Let $a := \arg(w - z)$ be the angle made by n with the positive x-axis. Then the gradient of l is $t_l := \tan(a - \theta/2)$ and the gradient of o is $t_o := \tan(a + \phi/2)$. Hence, the lines have equation

$$l : y = t_l(x - \operatorname{Re}(z)) + \operatorname{Im}(z) \qquad o : y = t_o(x - \operatorname{Re}(\omega)) + \operatorname{Im}(\omega)$$

Solving these simultaneously, we get

$$\operatorname{Re}(p) = \frac{t_l \operatorname{Re}(z) - \operatorname{Im}(z) - t_o \operatorname{Re}(\omega) + \operatorname{Im}(\omega)}{t_l - t_o}$$

$$\operatorname{Im}(p) = \frac{t_l t_0(\operatorname{Re}(z) - \operatorname{Re}(\omega)) + t_l \operatorname{Im}(\omega) - t_0 \operatorname{Im}(z)}{t_l - t_o}$$

These formulas are not particularly elegant but they are easily calculated by a computer. □

Corollary 2.1.1. *Let $R_p^\alpha = R_\omega^\phi \circ R_z^\theta$, with $\theta, \phi \in \pi\mathbb{Q}$ and $\theta + \phi \notin 2\pi\mathbb{Z}$. Then R is a rotation with $\alpha \in \pi\mathbb{Q}$. That is, the composition of rational rotations is a rational rotation (or translation).*

This is especially useful for overlapping disc rotations, because it means that if the initial rotation angles are rational, then points will only ever experience rational rotations. Furthermore, if θ and ϕ can both be expressed in the form $\pi m/n$ with $m, n \in \mathbb{Z}$, then any sequence of the initial rotations always produces a new rotation angle of $\pi k/n$, with $k \in \mathbb{Z}$, so the angle of rotation is bounded from below by π/n.

3 Properties of $\mathcal{E}_T$

Using Python [Van Rossum and Drake, 2009], we can generate images of the exceptional set for values of θ, up to some resolution and finite number of iterations. For each pixel in the image, we repeatedly map the corresponding point in the complex plane by the inverse of T^θ, forming the set $\{(T^\theta)^n(z)\}$. If any iterate is within some δ of the atom boundaries that would induce a discontinuity, we colour the pixel black [Smith et al., 2019]. Figure 3 gives two examples, with more in the appendix. Technically, we are only calculating $\mathcal{E}_T^+$ here, but we will show that this is sufficient for visualising $\mathcal{E}_T$ as a whole.

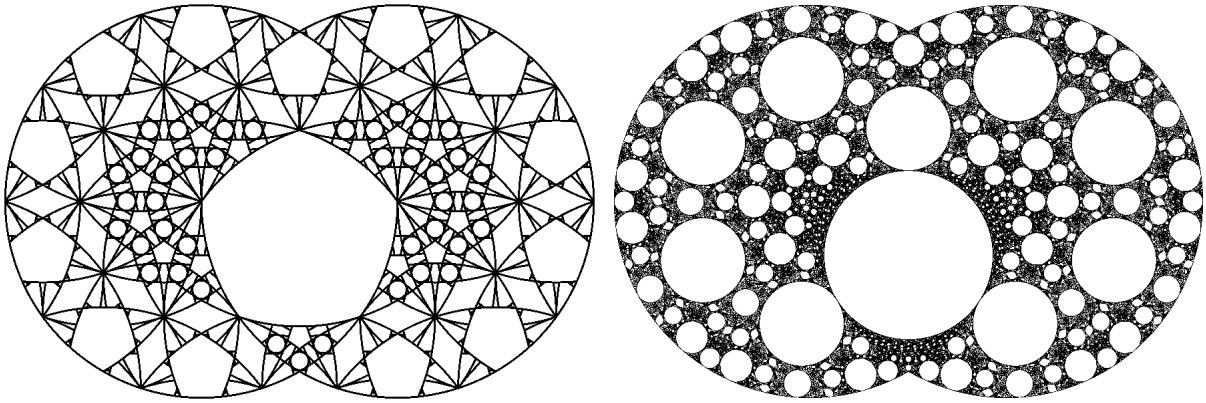

Figure 3: Two images of $\mathcal{E}_T$. Left: $\theta = \pi/5$, 150 iterations. Right: $\theta = 1$, 300 iterations.

Lemma 3.1. *The exceptional set $\mathcal{E} := \mathcal{E}_T$ is symmetric about* $\mathrm{Re}(z) = 0$

Proof. Let R_1, R_2 be the rotations R_1^θ and R_2^θ and σ the reflection about the central vertical $\mathrm{Re}(z) = 0$. We observe that $R_1 = \sigma R_2^{-1}\sigma$. Similarly, we have $R_2 = \sigma R_1^{-1}\sigma$. Hence,

$$T = R_2R_1 = \sigma R_1^{-1}\sigma\sigma R_2^{-1}\sigma = \sigma R_1^{-1}R_2^{-1}\sigma = \sigma T^{-1}\sigma$$

Hence, $T^n = \sigma T^{-n}\sigma$ and $T^{-n} = \sigma T^n\sigma$. Furthermore, $T^{-n}(\sigma z) = (\sigma T^n\sigma)(\sigma z) = \sigma T^n(z)$. Now, suppose $z \in \mathcal{E}$, and so T^n is discontinuous at z for some $n \in \mathbb{Z}$. That is, $\exists \varepsilon_0 > 0$ such that for all $\delta > 0$, $\exists z_\delta \in B(z, \delta)$ such that $|T^n(z) - T^n(z_\delta)| > \varepsilon_0$. Hence, for all $\delta > 0$ there is a $z_\delta \in B(z, \delta)$ such that

$$|T^{-n}(\sigma z) - T^{-n}(\sigma z_\delta)| = |\sigma T^n(z) - \sigma T^n(z_\delta)| = |T^n(z) - T^n(z_\delta)| > \varepsilon_0$$

Therefore, T^{-n} is discontinuous at σz.
Hence $z \in \mathcal{E} \implies \sigma z \in \mathcal{E} \implies z \in \sigma\mathcal{E}$, so $\mathcal{E} \subseteq \sigma\mathcal{E}$. Using a very similar proof, we can show that $T^n(\sigma z) = \sigma T^{-n}(z)$, which gives $\sigma\mathcal{E} \subseteq \mathcal{E}$. Finally, we get $\mathcal{E} = \sigma\mathcal{E}$, and so $\mathcal{E}$ is reflective about $\mathrm{Re}(z) = 0$. This symmetry is clearly displayed in the sets shown in Figure 3. □

Lemma 3.2. *Two points in $D \setminus \mathcal{E}$ have the same itinerary if and only if they are connected in $D \setminus \mathcal{E}$.*

Proof. Suppose $\theta \in 2\pi\mathbb{Z}$. Then both rotations are the identity and $\mathcal{E} = \emptyset$, so the claim is true. Otherwise, suppose $\theta \notin 2\pi\mathbb{Z}$ and consider two points with different itineraries. That is, for some $n \in \mathbb{Z}$ and two points $z_1, z_2 \in D \setminus \mathcal{E}$, $T^n(z_1)$ and $T^n(z_2)$ are in different atoms, and so when applying T one more time, they experience distinct isometries. Consider a continuous path $\gamma : [0,1] \to D$ with $\gamma(0) = z_1$ and $\gamma(1) = z_2$. From above, we get that $T^{n+1}(z_1)$ and $T^{n+1}(z_2)$ experience different isometries. Hence, $\exists t \in (0,1)$ such that $\forall \varepsilon > 0$, then $\gamma(t-\varepsilon)$ and $\gamma(t+\varepsilon)$ experience distinct isometries under T^{n+1}. This means there is a discontinuity at $\gamma(t)$ under T^{n+1}, and hence $\gamma(t) \in \mathcal{E}$. That is, for any path from z_1 to z_2, at least one point on the path is in the exceptional set, and hence the two points are disconnected in $D \setminus \mathcal{E}$. On the other hand, suppose two points are connected. That is, $\exists \gamma$ as before, such that $\gamma \subseteq D \setminus \mathcal{E}$. Hence, there is no n for which T^n introduces a discontinuity in γ. That is, they remain in the same atom (otherwise a discontinuity will be introduced). Hence, the two points share the same itinerary for every value of $n \in \mathbb{Z}$. □

Corollary 3.2.1. *Maximally connected subsets of $D \setminus \mathcal{E}$ are exactly those maximal subsets that share the same itinerary. Hence, islands and cells are equivalent in this system.*

This shows that the islands we see in the generated images form a one-to-one equivalence with the theoretical *cells* that have been a focus of previous study of piecewise isometries [Goetz, 2003]. Furthermore, it shows that to evaluate the movement of islands about the system, we only need to choose a representative from each island, and in turn each of these representatives will exhibit a different itinerary.

Lemma 3.3. *Every non-degenerate island has a periodic orbit. That is, for any non-empty, maximally connected open subset $I \subseteq D \setminus \mathcal{E}$, there is a $k \in \mathbb{N}$ such that $T^k(I) = I$.*

Proof. As I is non-degenerate, it has a positive Lebesgue measure (area). Consider each set $T^n(I)$. Because I is an island, every point in I shares the same itinerary, and so each $T^n(I)$ is connected. Furthermore, T^n acts as an isometry on I, and so $\mu(I) = \mu(T^n(I))$ for all $n \in \mathbb{N}$. By the Pigeonhole Principle, $\exists m, n \in \mathbb{N}$ with $m < n$ such that $T^m(I) \cap T^n(I) \neq \emptyset$. Because T is bijective, we can set $k := n - m$ and so $I \cap T^k(I) \neq \emptyset$. Consider some $z \in I \cap T^k(I)$. Since every point in an island has the same itinerary, every point in both I and $T^k(I)$ have the same itinerary. Because islands are maximal subsets of points of the same itinerary, then $T^k(I) = I$. □

Lemma 3.4. *If $\theta \in \pi\mathbb{Q}$, then every point $z \in \mathrm{Int}(D \setminus \mathcal{E})$ has periodic orbit.*

Proof. Let $z \in \mathrm{Int}(D \setminus \mathcal{E})$. Then z belongs to some non-degenerate island I. By Lemma 3.3, $\exists k \in \mathbb{N}$ such that $T^k(I) = I$. If T^k restricted to I is the identity transformation, then z has periodic orbit. Otherwise, since T^k fixes I and is a non-identity, orientation-preserving isometry, it must be a rotation fixing a point in I. Furthermore, this rotation is rational by Corollary 2.1.1. Hence, we can find an m such that T^{mk} restricted to I is the identity map (with rotation angle $\phi \equiv 0 \pmod{2\pi}$). Hence, $T^{mk}(z) = z$, and so the orbit of the point is periodic. □

Remark. This lemma is not true in general for $\theta \notin \pi\mathbb{Q}$. Every island has a periodic orbit, but points within an island may be rotated by an irrational amount (as the transformation is a composition of irrational rotations). Hence, points do not necessarily ever return back to where they began within the island.

Corollary 3.4.1. *For some island $I \subseteq D$, let k be minimal such that $T^k(I) = I$. If $\theta \in \pi\mathbb{Q}$, then T^k will rotate I by some amount $\pi m/n$, with $\gcd(m, n) = 1$. Then I has degree-n rotational symmetry.*

This corollary explains the appearance of regular polygons, with sides comprised of circle arcs that can be seen on the left image of Figure 3, and in the exceptional sets shown in the appendix.

Corollary 3.4.2. *Furthermore, if $\theta \notin \pi\mathbb{Q}$, then $\mathrm{Int}(D \setminus \mathcal{E})$ is a disjoint union of open discs. Because each rotation angle is irrational, we never get finite-sided polygons periodic under T.*

Lemma 3.5. *Let $\overline{S}$ be the Euclidean closure of a set S. Then $\overline{\mathcal{E}^+} = \overline{\mathcal{E}}$, where $\mathcal{E}^+$ is the forward exceptional set.*

Proof. Let $\mathcal{E}^-$ be the backward exceptional set. Then $\mathcal{E} = \mathcal{E}^- \cup \mathcal{E}^+$. It remains to prove that $\overline{\mathcal{E}^-} = \overline{\mathcal{E}^+}$. Suppose that $z \in \overline{\mathcal{E}^-}$. Hence, $\forall \delta > 0$ we have $B(z, \delta) \cap \mathcal{E}^- \neq \emptyset$, and hence $\exists y \in B(z, \delta)$ such that $y \in \mathcal{E}^-$. Therefore, we can find an $n \in \mathbb{N}$ such that $T^{-n}(y) \in \mathcal{E}_0$, and so $y \in T^n(\mathcal{E}_0)$, where $\mathcal{E}_0$ is the 'cut lines', or the boundary between the atoms. Now, suppose $z \notin \overline{\mathcal{E}^+}$. Then there exists some maximally connected, open set $A \subset D$ such that $z \in A$ and $A \cap \overline{\mathcal{E}^+} = \emptyset$. By definition, $\forall n \in \mathbb{N}$, $T^n(A) \cap \mathcal{E}_0 = \emptyset$. That is, A is never 'cut' during its orbit, and T^n always acts on A by isometry. By Lemma 3.3, we know that A will have a periodic orbit, and there is some positive integer m such that $T^m(A) = A$.
Since A is open, there exists an $\varepsilon > 0$ such that $B(z, \varepsilon) \subseteq A$. Letting $\delta = \varepsilon$, we have $y \in A$, and hence $A \cap T^n(\mathcal{E}_0) \neq \emptyset$. Now suppose k is an integer such that $km \geq n$. Hence, $T^{km}(A) \cap T^n(\mathcal{E}_0) \neq \emptyset$. As T is bijective, we can apply the inverse to get $T^{km-n}(A) \cap \mathcal{E}_0 \neq \emptyset$, and hence $A \cap \mathcal{E}^+ \neq \emptyset$. This is true for all $\varepsilon > 0$, and so we derive a contradiction. Hence, $z \in \overline{\mathcal{E}^+}$. This implies that $\overline{\mathcal{E}^-} \subseteq \overline{\mathcal{E}^+}$. We can use a similar proof to show the reverse implication and so we can derive that $\overline{\mathcal{E}^-} = \overline{\mathcal{E}^+}$, which completes the proof. □

4 Bounding Itineraries

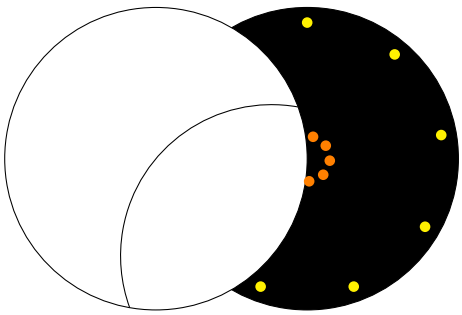

Figure 4: The orbit of points in atom 2 under R_2^θ close and far from the centre of the circle.

Let $T = R_2^\theta \circ R_1^\theta$ with $\theta \in [0, \pi]$. This restriction is possible because if $\theta \in (\pi, 2\pi)$, the system acts identically by taking $2\pi - \theta$ and reflecting about the x-axis. We wish to establish some rules which limit the possible itineraries points can have under T. This governs possibilities which can be used to create bounds when

enumerating itineraries. Recall that the atoms and their corresponding transformations in our system are:

$$0 : R_2^\theta \circ R_1^\theta \qquad 1 : R_1^\theta \qquad 2 : R_2^\theta$$

In complete generality, the itinerary of every point can be written in the following form:

$$\ldots 2^{c_2} 1^{b_2} 0^{a_2} 2^{c_1} 1^{b_1} 0^{a_1} 2^{c_0} 1^{b_0} 0^{a_0}$$

Each of the exponents are non-negative integers and exactly one of a_k, b_k, c_k are non-zero for each $k \in \mathbb{Z}$.

Lemma 4.1. *Suppose in the itinerary of a point, $b_i > 0$ or $c_i > 0$. Let k be the positive value. Then:*

$$\left\lceil \frac{\pi}{\theta} \right\rceil \leq k \leq \left\lceil \frac{5\pi}{3\theta} \right\rceil$$

Proof. Suppose $k = c_i > 0$. We want to bound how many times a point can stay in atom 2. That is, we want to bound the number of points of the form $re^{n\theta i} + 1$ we can fit inside atom 2, for $r \in [0, 2]$.

Consider Figure 4 showing the orbits of points close to the centre and close to the boundary of the second disc, in which atom 2 is contained. If we consider a point arbitrarily close to the centre, we can treat the boundary of the left circle as a vertical line. That is, we can fit points within a rotation of π. On the outside, the first disc intersects the second at an angle of $\pi/3$, and hence the reflex angle around the boundary of the circle is $5\pi/3$. Hence, we infer that

$$\left\lceil \frac{\pi}{\theta} \right\rceil \leq k \leq \left\lceil \frac{5\pi}{3\theta} \right\rceil$$

The ceiling function is used because as long as there is room left to rotate, the point is still in atom 2. We have a similar diagram if $b_i > 0$, looking at rotations around atom 1. Hence, we can bound the number of times any point stays in atom 1 or 2. Furthermore, this shows that atoms 1 and 2 have no fixed points if $\theta \notin 2\pi\mathbb{Z}$. □

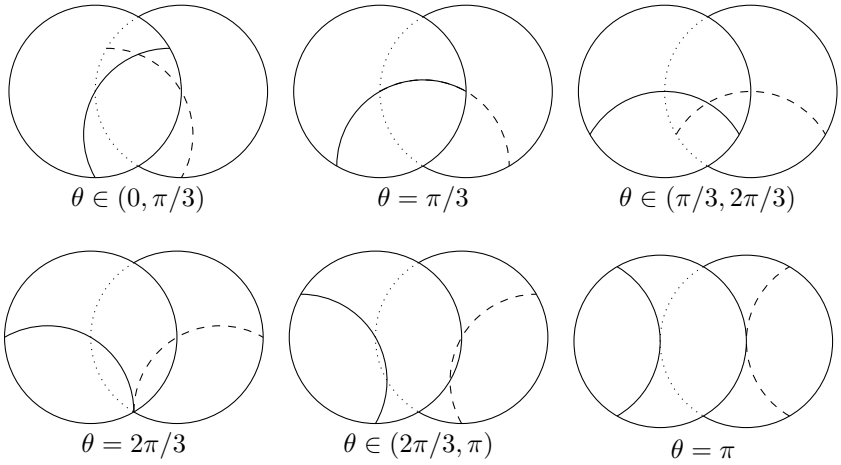

Figure 5: Atom 0 and its image for various values of θ

	0	1	2
0	✓	✓	✓
1	✓	✓	×
2	✓	✓	✓

	0	1	2
0	✓	×	✓
1	✓	✓	×
2	✓	✓	✓

	0	1	2
0	✓	✓	✓
1	✓	✓	×
2	✓	✓	✓

	0	1	2
0	×	✓	✓
1	✓	✓	×
2	✓	✓	✓

	0	1	2
0	×	✓	✓
1	✓	✓	×
2	✓	✓	✓

	0	1	2
0	×	✓	×
1	✓	✓	×
2	×	✓	✓

Figure 6: Tables for each θ (matching Figure 5), showing which mappings between atoms are possible.

We can also determine which atoms map into which other atoms. For example, for which values of θ contain some $z \in D \setminus \mathcal{E}$ such that z is in atom 0 and $T^\theta(z)$ is in atom 2. We visualise these possibilities in Figure 5, showing the region of atom 0 (bounded by the solid line), and its image (bounded by the dashed line). Using these, we can create a table which gives the possible maps between atoms for each of these ranges of θ, which can then be compared. The tables in Figure 6 are ordered the same as in Figure 5. The rows give the originating atom and the columns give the atoms after applying T^θ. If there is a cross, then there is no point in the originating atom that maps into the resulting atom. For example, no point in atom 1 ever maps to atom 2.

5 Further Generalisations

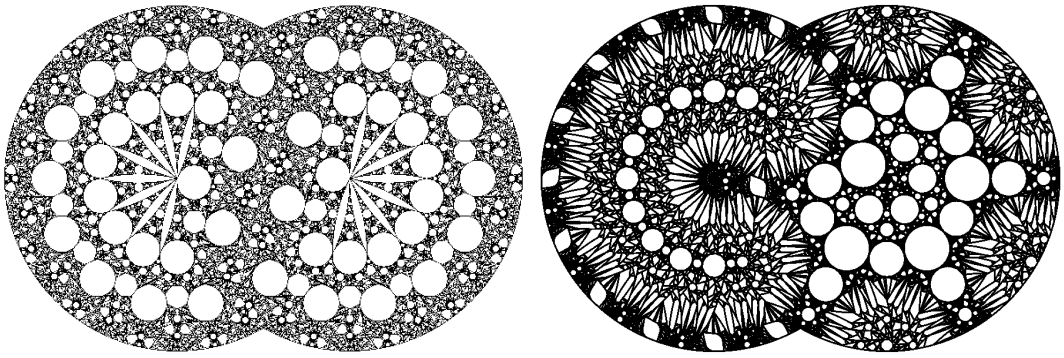

Figure 7: Left: $\theta_1 = \pi/7$, $\theta_2 = -\pi/7$, 300 iterations. Right: $\theta_1 = \pi/8$, $\theta_2 = -\pi/3$, 150 iterations.

The overlapped disc system has many possible generalisations, which all give rise to unique geometric properties. Depending on the modification, some of the previously-proven properties can be directly carried over and inferred, whereas others may require alteration or abandonment. For example, suppose we perform rotations of θ in the left circle and $-\theta$ in the right. An example is given in Figure 7 on the left. There is no

longer a symmetry about $\mathrm{Re}(z) = 0$. Instead, we replace the statement $R_1 = \sigma R_2^{-1} \sigma$ with $R_1 = \rho R_2^{-1} \rho$, where ρ is a rotation of π about $z = 0$. The same symmetry arguments as before are used to show $\mathcal{E} = \rho\mathcal{E}$, and hence the exceptional set has rotational symmetry of π about $z = 0$. When we have two rotation angles $|\theta_1| \neq |\theta_2|$, this symmetry is entirely broken, as demonstrated on the right panel of Figure 7. However, each circle still may exhibit partial rotational symmetry outside of the intersection of the two circles.

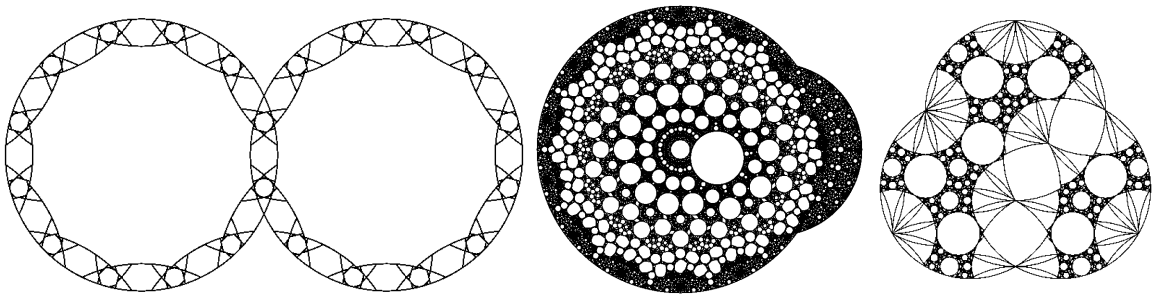

Figure 8: Left: $\theta = \pi/6$, $d = 1.8r$. Middle: Different disc sizes. Right: A three-disc system.

Furthermore, we can move and adjust the sizes of our discs, as well as the rotation angles. Moving the circles further apart restricts the exceptional set to annuli within each of the two discs. If $\theta_1 = \pm\theta_2$, the reflection/rotation symmetry still remains. In all of these systems, non-degenerate islands still have finite periods and if the rotation angles are all rational, then each point in $\mathrm{Int}(D \setminus \mathcal{E})$ will have a periodic orbit. In the three-disc case, there appear to be additional (albeit more complex) symmetries present, although these depend on the angles chosen. For example, we appear to get reflective symmetry about *one* of the 'natural axes' through the centre and a point of intersection, but not about the other two.

6 Extending to 3D

A further generalisation is to consider alternate rotations of two intersecting spheres centered at the coordinates $(1, 0, 0)$ and $(-1, 0, 0)$ with radius 2 [Smith et al., 2019]. In fact, most of the cases of the overlapped disc rotation system are fully encapsulated within this 3D case. There are also extra degrees of freedom from choosing both the angles of rotation and the directions of the axes of rotation.

In the case of parallel rotation axes, consider intersecting the spheres with a plane orthogonal to the axes and passing through the centres of the spheres. This plane is invariant under each of the the two rotations, and the dynamics of the system on the plane is identical to the 2D overlapping disc rotations first discussed. If we move the plane along the rotation axes, the dynamics become equivalent to the system with separated discs. Skewing and moving the rotation axes (but keeping them parallel) gives the case where one circle is larger than the other on the intersecting plane, and so these 2D cases are covered by rotations on parallel axes of the spherical system (without changing the size or placement of the spheres).

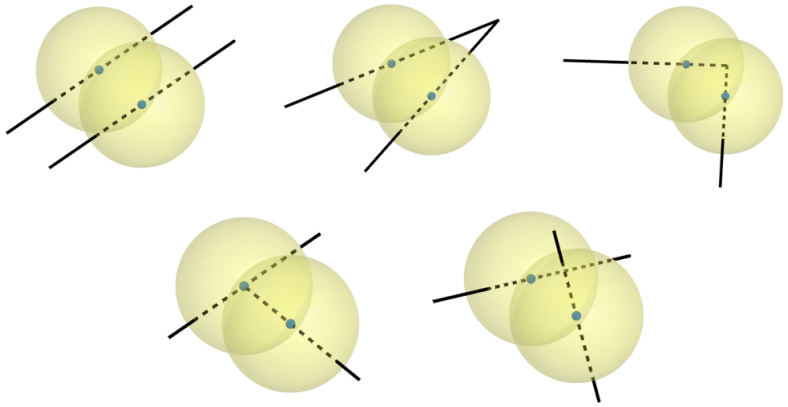

Figure 9: A compilation of cases for rotations of two spheres about independent axes.

Suppose the two axes are no longer parallel, and intersect at the point $(0, a, 0)$. A sphere centered at this point will be invariant under both of our rotations. If the sphere has radius $\sqrt{1+a^2}$, it will intersect the centres of the two original spheres. As $a \to \infty$, the system approaches the 2D case with parallel axes. We now visualise the exceptional set of this system under $T = R_2^{\theta_2} \circ R_1^{\theta_1}$, and $\theta_1 = \theta_2 = \pi/3$ using the Lambert Azimuthal Equal-Area Projection [Mulcahy, 1997], facing toward the sphere from the origin.

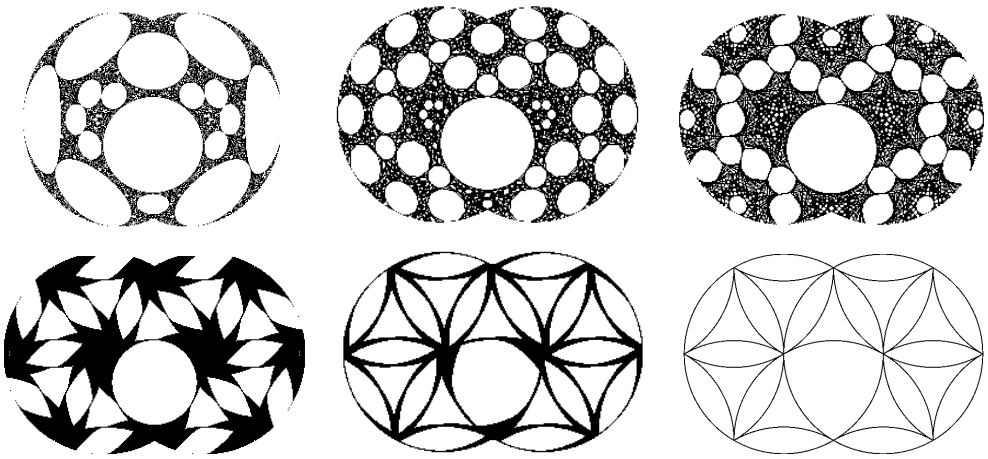

Figure 10: Exceptional sets for $\theta = \pi/3$, 300 iterations. Axes intersect resp. at $a = 1, 2, 3, 10, 30, \infty$.

As a increases, the domain approaches two 'true' circles. While a is finite, this system is fundamentally different to the 2D case due to the inherent curvature of the sphere, altering the shape of the domain on any projection we choose. In the second-to-last image of Figure 10, we can see the exceptional set for $\theta = \pi/3$ in the 2D case beginning to emerge. However, if we increased the number of iterations, the rest of the domain may fill up more as the lines do not return exactly to where they started due to the curvature.

If the axes are orthogonal, some of the invariant spheres will be small enough to fit entirely within the union of the two original spheres. Again, this is a fundamentally different system to the 2D case. In this case we only have two atoms for our rotation, because every point in the sphere is rotated by the sphere it is contained within. Again, we can use the Lambert projection to visualise the exceptional set on a disc. An example is given in the appendix. If the axes are skew (that is, non-parallel and non-intersecting), there is no invariant surface we can take. Hence, it is not possible to project this system onto any 2D system. A 3D exceptional set can be calculated and displayed as a 3D object, but its structure would be difficult to visualise and interpret.

7 Tilings and the Full Exceptional Set

In order to show that a tiling of cells is finite for any sequence of rotations by particular angles, we can calculate the full exceptional set $\mathbf{E}_{\mathbb{T}}$. First, we must restate the definition of the exceptional set in an equivalent but different way:

$$\mathbf{E}_{\mathbb{T}} = \bigcup_{T \in \mathbb{T}} T(\mathcal{E}_0)$$

Here, $\mathbb{T}$ is the set of all combinations of rotations and $\mathcal{E}_0$ are the original 'cutting lines' that form the boundaries between the atoms of the transformation. An easy way to determine this full set is to extend those initial lines to full circles (rather than arcs), and map the circles under the rotations. Hence, we only have to consider mapping the centres of the circles, rotating those centres when the circle at that centre intersects the circle we are rotating. We can hence generate $\mathbf{E}_{\mathbb{T}}$ with the following recursive algorithm:

- Let $S_0 = \{-1, 1\}$
- Let $S_{n+1} = S_n$.
  For each $s \in S_n$, if $|s + 1| \leq 4$, add $R_1^{\theta}(s)$ to S_{n+1}. Similarly, if $|s - 1| \leq 4$, add $R_2^{\theta}(s)$ to S_{n+1}.
- Let S_n° be the set of circles of radius 2 centered at S_n.

We then have $\mathbf{E}_{\mathbb{T}} = \lim_{n\to\infty}(S_n^{\circ} \cap D') = D' \cap \lim_{n\to\infty}(S_n^{\circ})$, where D' is the extended domain, consisting of the union of discs centered at 1 and -1 of radius four, rather than radius two. If $\lim_{n\to\infty} |S_n|$ is finite, then $S_{n_0+1} = S_{n_0}$ for some $n_0 \in \mathbb{N}$. Furthermore, the number of regions that $\mathbf{E}_{\mathbb{T}}$ divides D into must be finite, and hence for any $T \in \mathbb{T}$, there must be finite islands remaining after removing the set $\mathcal{E}_T$. Finally, all of these islands will be non-degenerate. For $\theta \in \{2\pi, \pi, \pi/2, \pi/3, 2\pi/3\}$, we can explicitly construct the sets $\lim_{n\to\infty} S_n$. These are shown in Figure 11, and all are finite.

Lemma 7.1. *Let $S := S_\infty$ be the set of centres of circles that contribute arcs to $\mathbf{E}_{\mathbb{T}}$. Let R_1 and R_2 be rotations by θ around the circles centered at -1 and 1. Then S has the following properties:*

1. $\{-1, 1\} \subseteq S$
2. $R_1(\{s \in S \,|\, |s + 1| \leq 4\}) = \{s \in S \,|\, |s + 1| \leq 4\}$
3. $R_2(\{s \in S \,|\, |s - 1| \leq 4\}) = \{s \in S \,|\, |s - 1| \leq 4\}$

Corollary 7.1.1. *If $\theta \notin \pi\mathbb{Q}$, then $|S| = \infty$, and so $\mathbf{E}_\mathbb{T}$ divides D into countably infinite regions.*

Proof. We have that $1 \in S$. Since $|1 + 1| \leq 4$, we rotate the point 1 around the left circle by θ. We can keep applying R_1 without losing the inequality, so we have:

$$\left\{e^{k\theta i} - 1 \,\middle|\, k \in \{1, \ldots, n_0\}\right\} \subseteq S_{n_0}$$

Because $\theta \in \pi(\mathbb{R}\setminus\mathbb{Q})$, this will generate a new point for each n. Hence, there is no n_0 for which $S_{n_0+1} = S_{n_0}$. □

Corollary 7.1.2. *If $\theta \in \{2\pi, \pi, \pi/2, \pi/3, 2\pi/3\}$, then $D \setminus \mathbf{E}_\mathbb{T}$ has finite islands.*

We will not give a full proof of the corollary here, but in the figure we give the set S for each θ. It can be seen that they will be invariant under the rotations. Lines are drawn between the points to highlight their connections to Euclidean tilings of space [Grünbaum and Shephard, 1977].

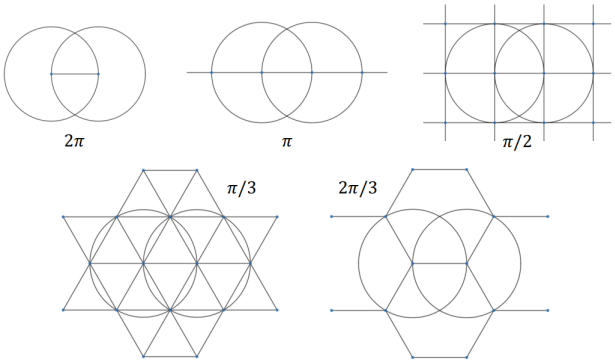

Figure 11: Sets S_∞ for $\theta = \pi m/n$ and $n \leq 3$, with their corresponding tilings.

Each of these contains only finite circle centres, and hence $D \setminus S^\circ$ will be finite, and so the domain after removing $\mathcal{E}$ contains only finitely many islands, all of which must be non-degenerate.

Conjecture 7.2. Let $\theta \in \pi\mathbb{Q}$, such that $\theta = \pi m/n$ with $\gcd(m, n) = 1$. Then $|S| = \infty \iff n > 3$.

By using the contrapositive, we have already proved this conjecture in one direction. We aim to prove a somewhat weaker version in the other direction, which hopefully leads to a full proof. To this, we construct a new set $\mathbf{S} \supseteq S$ which follows the same rules as S, except we do not limit when we rotate centres. Hence, we want a set with the following properties:

1. $\{-1, 1\} \subseteq \mathbf{S}$
2. $R_1(\mathbf{S}) = \mathbf{S}$
3. $R_2(\mathbf{S}) = \mathbf{S}$

Except for the case $\theta = 2\pi$, the set $\mathbf{S}$ is necessarily infinite. However, if we can prove that $|\mathbf{S} \cap D'|$ is (in)finite, then we may be able to prove the same for S.

Lemma 7.3. *If $\theta = \pi m/n$, then every point $s \in \mathbf{S}$ has rotational symmetry of θ/n around it.*

Proof. Let $s \in \mathbf{S}$. Then, there is some sequence of rotations $R \in \{R_1, R_2\}^*$ such that either $s = R(1)$ or $s = R(-1)$. Suppose we are in the latter case. Since $\theta = \pi m/n$, and $\gcd(m, n) = 1$, then there is some positive integer k such that:

$$k\theta \pmod{2\pi} \equiv \frac{km\pi}{n} \pmod{2\pi} \equiv \frac{\pi}{n} \pmod{2\pi}$$

Now, consider the transformation $T = RR_1^k R^{-1}$. We have that $T(s) = RR_1^k(-1) = R(-1) = s$, so $T(s)$ fixes s. Since this transformation is a composition of rotations fixing a point, it is also a rotation. We can see that the effect of T on $\mathbf{S}$ will be a rotation by π/n around s. Since R_1^{-1} and R_2^{-1} can be written in terms of R_1 and R_2 for $\theta \in \pi\mathbb{Q}$, then $T \in \{R_1, R_2\}^*$, completing our proof. □

Lemma 7.4. *Let $\mathbf{S}_1$ be the set of points $s \in \mathbf{S}$ if there exists an $R \in \{R_1, R_2\}^*$ such that $R(1) = s$. Then $\mathbf{S}_1 + (s' - s'') = \mathbf{S}_1$ for any $s', s'' \in \mathbf{S}_1$.*

Proof. The proof proceeds similarly as before. Let R' be the sequence of rotations such that $R'(1) = s'$ and R'' such that $R''(1) = s''$. Then consider $T = (R')^{-1} R_1^k R''$, choosing k such that the total angle of rotation is a multiple of 2π. This is possible by our formula for composition of rotations and that $\gcd(m, n) = 1$. Hence, the transformation becomes a translation, mapping s' to s'', and since $\mathbf{S}_1$ is invariant under these rotations, we also must have $T(\mathbf{S}_1) = \mathbf{S}_1$. □

We are now ready to prove the 'weak' version of our conjecture.

Theorem 7.5. $\mathbf{S}$ *is locally finite if and only if $\theta = m\pi/n$ and $n \leq 3$.*

Proof. If $\theta \in \pi\mathbb{Q}$ and $n \leq 3$, then $\mathbf{S}$ corresponds to one of the Euclidean tilings shown in Figure 11, extended to the entire plane. If $\theta \notin \pi\mathbb{Q}$, we use Corollary 7.1.1, and since S is infinite inside a compact domain, then $\mathbf{S}$ is not locally finite. Finally, suppose that $\theta \in \pi\mathbb{Q}$ and $n > 3$. We have that $\mathbf{S}_1$ is invariant under translation between any two points in the set and has rotational symmetry of π/n about each point. Suppose that $\mathbf{S}_1$ is locally finite. The translational invariance about any point implies the conditions for a Euclidean tiling, with regular polygons with interior angle θ. However, such a polygon does not exist if $n > 3$, and so we derive a contradiction. That is, $\mathbf{S}_1$ is not locally finite and hence $\mathbf{S}$ is not locally finite. □

Now, consider the set $\mathbf{S} \cap D'$. Since D' is invariant under the rotations given in the construction of S, we know that S is a countable subset of D'. Furthermore, since the construction of $\mathbf{S}$ is a 'unrestricted' version of the construction of S, $\mathbf{S} \cap D' \supseteq S$. By the theorem, we have that $|\mathbf{S} \cap D'| < \infty$ if and only if $n \leq 3$, however this does not prove the theorem. The issue is that we may have points that end up in D' through this unrestricted construction but aren't in S because we must perform rotations when the point is too far from the rotation centre for this to be valid in S. It remains open to see if we can prove that $\mathbf{S} \cap D' = S$, or at least that $|S|$ will be infinite when $\mathbf{S}$ is. If this can be achieved, then the conjecture is proven.

8 Conclusion and Future Work

This paper gives a brief overview with computer-constructed visualisations of a collection of the geometric properties of overlapping disc rotations, a generalisation of the Cohan Circle puzzle. However, many properties remain left unproven and may require techniques and methods not discussed or shown here. For example, many of the proofs only work for non-degenerate islands. It seems reasonable that if θ is a rational rotation, then every island will be non-degenerate, whereas irrational angles will 'fill' the space. Furthermore, we could ask whether the closure of an exceptional set $\mathcal{E}_T$ has non-zero area (or more precisely, Lebesgue measure). As another extension of the proofs concerning periodic orbits, we could ask whether points in the exceptional set always have finite orbits for rational rotations. In general, finding a counterexample would be useful but difficult given the discontinuous nature of the transformations and the reliance on piecewise functions. Finally, future work would hopefully include finishing the proof of the conjecture, showing the relationship between $\mathbf{S} \cap D'$ and S. It also may be interesting to relate the full exceptional set to the sets $\mathcal{E}_T$ depending on the transformation chosen, and determining which of these lead to an infinite number of islands.

References

[Goetz, 2000] Goetz, A. (2000). Dynamics of piecewise isometries. *Illinois J. Math.*, 44(3):465–478.

[Goetz, 2003] Goetz, A. (2003). Piecewise isometries—an emerging area of dynamical systems. In *Fractals in Graz 2001*, Trends Math., pages 135–144. Birkhäuser, Basel.

[Grünbaum and Shephard, 1977] Grünbaum, B. and Shephard, G. C. (1977). Tilings by regular polygons. *Mathematics Magazine*, 50(5):227–247.

[Krotter et al., 2012] Krotter, M. K., Christov, I. C., Ottino, J. M., and Lueptow, R. M. (2012). Cutting and shuffling a line segment: mixing by interval exchange transformations. *Internat. J. Bifur. Chaos Appl. Sci. Engrg.*, 22(12).

[Mulcahy, 1997] Mulcahy, K. (1997). Cylindrical projections. http://www.geo.hunter.cuny.edu/mp/cylind.html. Accessed on 20-02-2020.

[Nortmann, 2002] Nortmann, A. (2002). Cohan circle. https://twistypuzzles.com/cgi-bin/puzzle.cgi?pkey=2569. Accessed on 20-02-2020.

[Smith et al., 2019] Smith, L. D., Umbanhowar, P. B., Lueptow, R. M., and Ottino, J. M. (2019). The geometry of cutting and shuffling: an outline of possibilities for piecewise isometries. *Phys. Rep.*, 802:1–22.

[Van Rossum and Drake, 2009] Van Rossum, G. and Drake, F. L. (2009). *Python 3 Reference Manual*. CreateSpace, Scotts Valley, CA.

9 Appendix

Exceptional sets of T^θ for various θ in the overlapped disc rotations system:

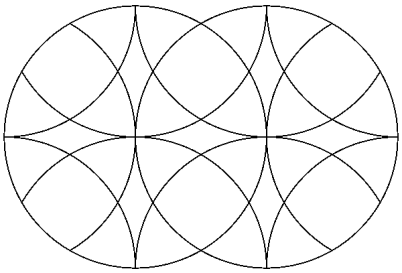

$\theta = \frac{\pi}{2}$

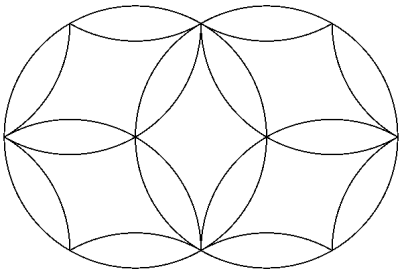

$\theta = \frac{3\pi}{2}$

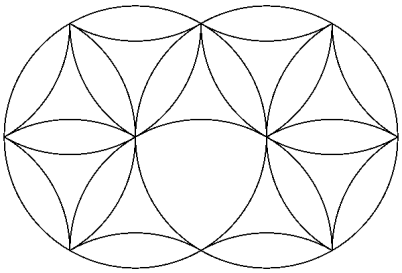

$\theta = \frac{\pi}{3}$

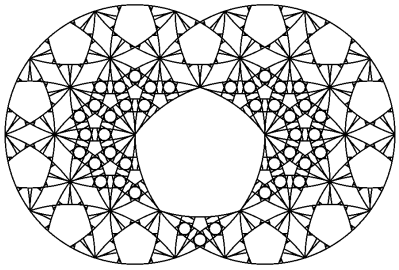

$\theta = \frac{\pi}{5}$

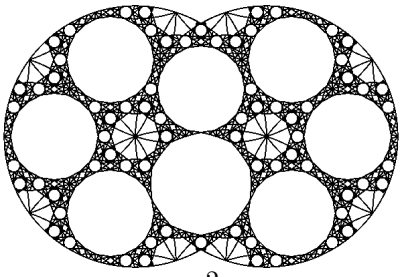

$\theta = \frac{2\pi}{5}$

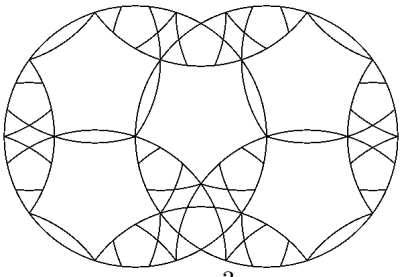

$\theta = \frac{3\pi}{5}$

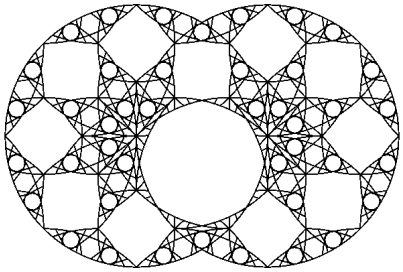

$\theta = \frac{\pi}{4}$

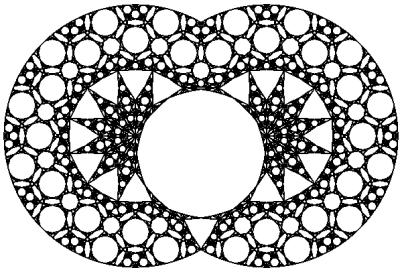

$\theta = \frac{\pi}{6}$

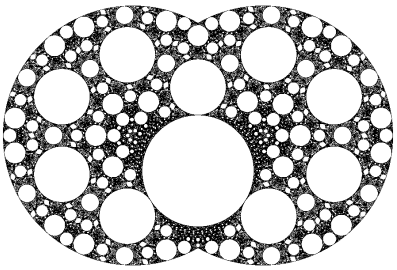

$\theta = 1$

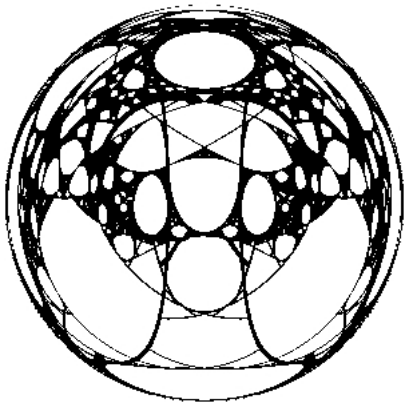

This is the exceptional set for the 3D case of rotations about orthogonal axes, intersecting at $(1, 0, 0)$. Both of the rotation angles are $\pi/6$. The exceptional set calculated is a subset of the sphere centered at $(1, 0, 0)$ with radius $\sqrt{2}$, projected from above using the Lambert Azimuthal Equal-Area Projection.